ACS APPLIED MATERIALS & INTERFACES

Research Article

www.acsami.org

Novel "Hot Exciton" Blue Fluorophores for High Performance Fluorescent/Phosphorescent Hybrid White Organic Light-Emitting Diodes with Superhigh Phosphorescent Dopant Concentration and Improved Efficiency Roll-Off

Xinhua Ouyang,[†] Xiang-Long Li,[‡] Ling Ai,[†] Dongbo Mi,[†] Ziyi Ge,*[,†] and Shi-Jian Su*[,‡]

[†]Ningbo Institute of Materials Technology and Engineering, Chinese Academy of Sciences, Ningbo 315201, P. R. China

[‡]State Key Laboratory of Luminescent Materials and Devices (South China University of Technology) and Institute of Polymer Optoelectronic Materials and Devices, South China University of Technology, Guangzhou 510640, P. R. China

Supporting Information

ABSTRACT: Two blue fluorophores with excellent hybridized local and charge-transfer (HLCT) and "hot exciton" properties were developed as the blue emitter and the host for orange-red phosphor to achieve highly efficient fluorescent/phosphorescent (F/P) hybrid white organic light-emitting diodes (WOLEDs) in a single-emissive-layer single-dopant (SEML-SD) architecture even at a high concentration of phosphorescent dopant. In the devices, part of the triplet excitons of the blue fluorophores can be utilized to realize reverse intersystem crossing from the triplet excited states to the singlet excited states for blue emission, and the diffusion volume range of the triplet excitons is reduced significantly. When the phosphorescent dopant concentration is up to 1.0 wt %, which is ten times higher than the traditional single-EML-SD F/P hybrid WOLEDs, highly efficient white emission was still achieved with maximum total external quantum efficiency (EQE) of 23.8%, current efficiency (CE) of 56.1 cd A^{-1}, and power efficiency (PE) of 62.9 lm W^{1-}. The results will supply a novel method for obtaining high efficiency F/P hybrid WOLEDs in a SEML-SD architecture with easily controllable doping concentration.

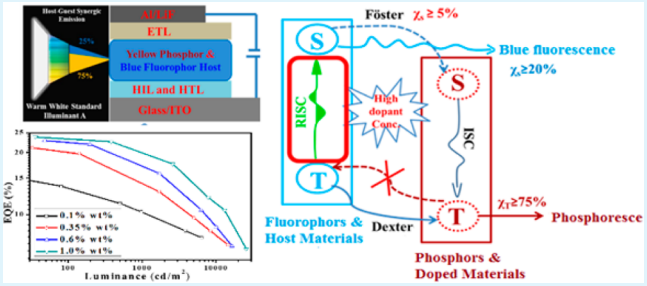

KEYWORDS: *hot exciton blue fluorophores, hybrid white organic light-emitting diodes, superhigh phosphorescent dopant concentration, improved efficiency roll-off*

1. INTRODUCTION

White organic light-emitting diodes (WOLEDs) are very significant owing to their potential applications in full-color displays and solid-state lighting.[1−3] Recently, fluorescent/phosphorescent (F/P) hybrid WOLEDs are thought as the best choice for WOLEDs because of their special advantages by combining the excellent stability of blue emitters and the high efficiency of phosphorescent emitters.[4−6] Currently, three typical architectures have been reported for F/P hybrid WOLEDs, including multiemissive-layer (MEML), single-emissive-layer with multidopant (SEML-MD), and single-emissive-layer with single-dopant (SEML-SD). Among these F/P hybrid WOLEDs, the device in a SEML-SD architecture has been considered to be as an effective approach to realize high efficiency with the reduced architectures and manufacturing process, as well as the possibility of decreasing or eliminating exciplex formation between the adjacent layers.[7,8]

For the SEML-SD F/P hybrid WOLEDs, the principal problem is yet focusing the separation and use of their singlet triplet and single excitons.[9] In order to achieve the 100% internal quantum efficiency, the idea model is to use the 25% singlet excitons by the blue emitters and the other 75% triplet excitons by the phosphorescent emitters. Thus, it will be required that the singlet excitons must be distributed exclusively to the blue emitters. However, singlet and triplet excitons are always formed together and recombined in the same place within the device. Therefore, a proper mechanism should be developed to effectively distribute the two different exciton species. In this regard, Forrest et al.[10] and Leo et al.[11] presented sequentially a suitable exciton management by diffusion based on the difference of singlet and triplet exciton diffusion length.[12] To achieve the harvesting of the triplet exciton, the blue emitter should be placed nearby the exciton generation zone, whereas phosphorescent emitter is located on the father distance, which ensures the fluorescent emission is completely from the singlet excitons and the phosphorescent emission is originated from the triplet excitons. Very recently, Zhang et al.[13] deepened the exciton diffusion mechanism to

Received: November 19, 2014
Accepted: March 31, 2015
Published: March 31, 2015

ACS Publications © 2015 American Chemical Society

DOI: 10.1021/am5081106
ACS Appl. Mater. Interfaces 2015, 7, 7869−7877

Scheme 1. Synthetic Route for the Compound PhBPI[a]

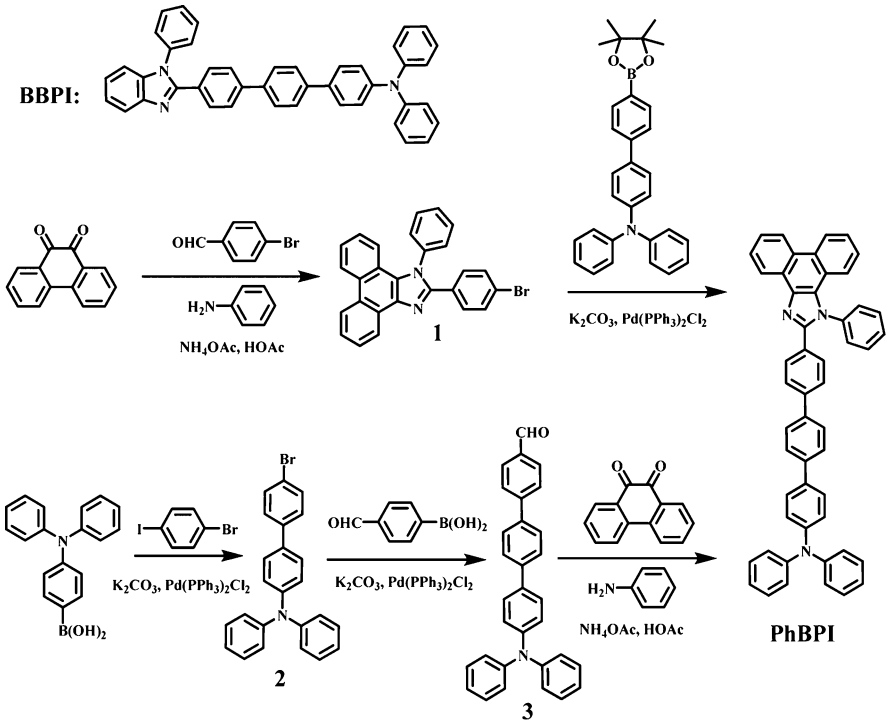

[a]Also shown the molecular structure of BBPI.

concentration regulation strategy. Their results showed the diffusion volume range of the singlet excitons is about 10 000 times smaller than that of the triplet excitons by considering the excitons in three-dimensional range. It means the phosphorescent dopant concentration should be very low (≤0.1 wt %). While the devices with so much low concentration of phosphorescent dopant will be difficultly fabricated in an accurate and constant doping concentration. Moreover, a small change of the concentration may give a significant effect on the performance of devices. Therefore, the development of SEML-SD F/P hybrid WOLEDs with improved doping concentration has been considered to be the currently important challenge for flexible manipulation.

For the traditional mechanism of the F/P hybrid WOLEDs, the concentration of the phosphorescent dopant is certainly low because of their exciton diffusion. To realize the high doping concentration, we may suppose if the conventional fluorophore could be replaced by the emitters with the abilities to realize reverse intersystem crossing from the triplet to the singlet excited states and thus utilize partial triplet excitons, like triplet−triplet annihilation (TTA),[14] thermally activated delayed fluorescence (TADF),[15] hybridized local and charge-transfer (HLCT)[16] and "hot exciton" processes.[17] Thus, a less 75% triplet exciton energies are transferred to the phosphor. In this way, the diffusion volume range of the triplet excitons should be no more 10000 times larger than that of the singlet excitons. To achieve the 100% internal quantum efficiency again, it must increase the capture of the triplet excitons in the diffusion volume, which means that the doping concentration of the phosphorescent emitter should be improved. As thus, the present dopant will not follow the conventional principle of the doping concentration rules. Herein, we demonstrated the first time about the single-EML-SD hybrid WOLEDs based on two blue emitters with HLCT and "hot exciton" properties. By employing BBPI and PhBPI as the blue emitter and the host of tris(2-phenylquinoline)iridium(III) ($Ir(2\text{-phq})_3$), the SEML-SD F/P hybrid WOLEDs exhibited excellent electroluminescene (EL) performance and improved efficiency roll-off with the maximal total current efficiency (CE), current efficiency (PE), and external quantum efficiency (EQE) of 56.1 cd A^{-1}, 62.9 lm W^{1-}, and 23.8%, respectively. Significantly, the present doping concentration of the phosphorescent emitter is raised to be a maximum value of 1.0 wt % versus the conventional one of 0.1 wt %, which further proves it is a feasible means to obtain the improved doping concentration of phosphorescent emitters for high performance F/P hybrid WOLEDs with a SEML-SD configuration.

2. RESULTS AND DISCUSSIONS

2.1. Synthesis, Thermal, and Electrochemical Properties. The synthesis of BBPI followed the method reported in literatures.[18] For PhBPI, two synthetic routes were envisioned in Scheme 1: either by Suzuki cross-coupling reaction of 2-(4-bromophenyl)-1-phenyl-1*H*-phenanthro[9,10-*d*]imidazole (**1**) and *N*,*N*-diphenyl-4′-(4,4,5,5-tetramethyl-1,3,2-dioxaborolan-2-yl)-[1,1′-biphenyl]-4-amine (route A) or treating 4″-(diphenylamino)-[1,1′:4′,1″-terphenyl]-4-carbaldehyde (**3**) with phenanthrene-9,10-dione (route B). For the route A, the important intermediate is compound **1** which was obtained through the condensation reaction of phenanthrene-9,10-dione with 4-bromobenzaldehyde and aniline. The similar polarities of the starting materials and PhBPI seriously affected the separation and purification processes, and thus satisfactory yield could not be achieved. Route B was proved to be attractive to access PhBPI with high yield and easy purification. The present novel products were identified by ^1H and ^{13}C NMR, MS, and EA (see Supporting Information). The compounds BBPI and PhBPI showed good thermal stability as exhibited by the decom-

DOI: 10.1021/am5081106
ACS Appl. Mater. Interfaces 2015, 7, 7869−7877

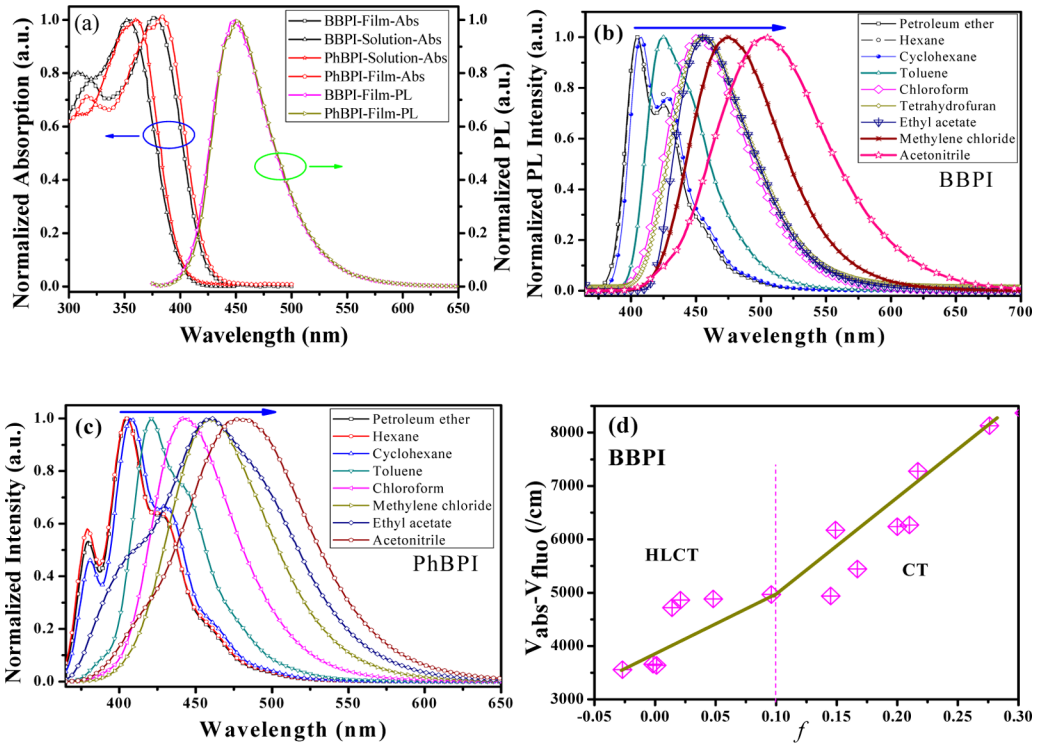

Figure 1. (a) Normalized UV−vis absorption and PL spectra of BBPI and PhBPI in chloroform solution and thin solid film state. (b) PL spectra of BBPI in solvents of different polarities. (c) PL spectra of PhBPI in solvents of different polarities. (d) Linear correlation of the orientation polarizability (Δf) of solvent media with the Stokes shift ($\nu_a - \nu_f$; a = absorbed light; f = fluorescence) for BBPI.

Table 1. Physical Parameters of the Compounds BBPI and PhBPI

	Abs[a] (nm)	PL[a] (nm)	T_g (°C)	T_d[b] (°C)	Φ[g] (%)	τ[h] (ns)	T_1[i] (eV)	HOMO (eV[c], eV[d])	LUMO (eV[c], eV[d])	E_g[e] (eV)	E_g[f] (eV)
BBPI	376	448	109	408	68	1.8	2.69	−5.28, −4.93	−2.33, −2.36	2.95	2.57
PhBPI	382	451	153	496	57	1.22	2.63	−5.20, −4.91	−2.30, −2.33	2.90	2.58

[a]UV−vis absorption and PL spectra in neat film. [b]Loss of 5 wt %. [c]HOMO was measured from the onset of oxidation potential; LUMO was deduced from HOMO and E_g. [d]Obtained from DFT calculations using B3LYP/6-31G(d,p). [e]Obtained from the onset of UV−vis absorption spectra in film. [f]Calculated from the HOMO and LUMO based on the calculations of B3LYP/6-31G(d,p). [g]Measured by the integrating sphere system with neat film. [h]τ is the fluorescence lifetime, measured on FLS920. [i]Triplet energy from phosphorescence spectra of THF solution at 77 K.

position temperatures (T_d, corresponding to 5% weight loss) of 408 and 496 °C (Supporting Information Figure S1) and the glass transition temperatures (T_g) of 103 and 154 °C as shown in the DSC curves (Supporting Information Figure S1 inset), respectively. The electrochemical properties of BBPI and PhBPI were measured by using cyclic voltammetry (CV). Their onset of oxidation (E_{ox} vs ferrocene/ferricenium) is 0.88 and 0.80 V (Supporting Information Figure S2), and correspondingly, their HOMO energy levels were calculated to be 5.28 and 5.20 eV, respectively.

2.2. Absorption and Photoluminescence (PL) Properties. The PL and UV−vis absorption spectra of BBPI and PhBPI were studied with various solvents and in thin solid film state, as shown in Figure 1 and Supporting Information Figure S3, respectively, and the important parameters are summarized in Table 1 and Supporting Information Table S1. Little changes were found in their absorption spectra with the increase of solvent polarity,which implied a little difference of dipolar on the ground state with different solvents. Both of them appearing around 355 and 300 nm can be respectively assigned to the internal charge transfer (ICT) transition and the n−π* transition. According to the onset of absorptions in film state, the optical band gaps (E_g) of BBPI and PhBPI are estimated to be 2.95 and 2.92 eV, respectively. Their fluorescence spectra are broadened and gradually red-shifted by increasing the polarity of solvent, as shown in Figure 1b and 1c, which indicate a big change of the dipole moment between the ground and the excited states. We plot the Stokes shift versus the orientation polarizability (Δf) as shown in Figure 1d and Supporting Information Figure S4. Obviously, two different excited states in high- and low-polarity solvents were found. The dipole moments were calculated to be 27.3 and 9.6 D for BBPI and 26.9 and 10.8 D for PhBPI. The present results are very similar to the pioneer work by Ma and his colleagues. Becaused of the similarity between this work and Ma and his colleagues, we can confirm these emitters also show the excited states of HLCT. Furthermore, their phosphorescent spectra and PL decay characteristics were also investigated as shown in Supporting Information Figures S5 and S6. The lifetimes of BBPI and PhBPI were observed to be 1.8 and 1.22 ns, respectively. Therefore, the emission from the BBPI and PhBPI can be attributed to the ordinary fluorescence.

2.3. Theoretical Calculation. To find the electronic transitions of BBPI or PhBPI, their singlet and triplet states containing the ground and excited states were evaluated by using Gaussian software at the level of B3LYP/6-31G (d,p) and

DOI: 10.1021/am5081106
ACS Appl. Mater. Interfaces 2015, 7, 7869−7877

TD-ωB97XD/6-31G (d,p) as shown in Figure 2. As far as the S_1 state is concerned, the hole and particle natural transition

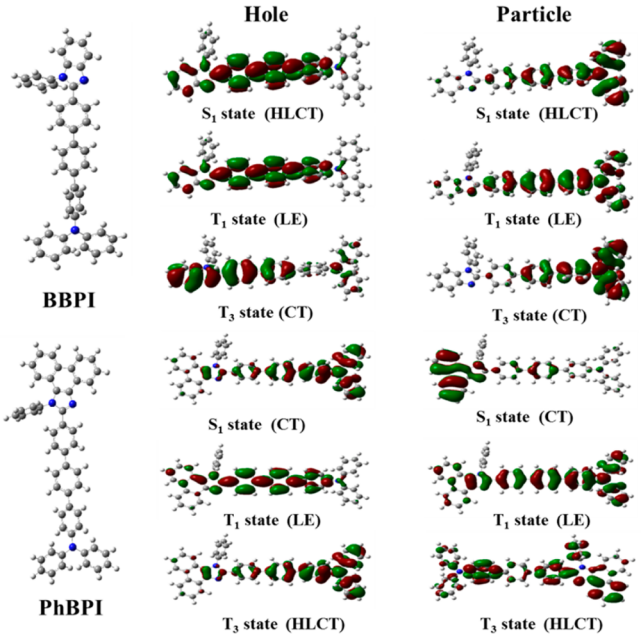

Figure 2. Geometric configurations and natural transition orbitals for S_1, T_1, and T_3 of BBPI and PhBPI.

orbitals (NTOs) show good balance between orbital overlap and spatial separation. The certain orbital overlaps exhibit local characters of their excited states. In the meanwhile, the existence of two components (CT and LE) are found by analyzing the calculated results, which is in good agreement with the results of the HLCT states. Considering the "hot exciton" process, we also calculate their low-lying triplet excited states T_1, second-lying triplet excited states T_2, and the third-lying triplet excited states T_3. Interestingly, a similar electron density is found beteween the high-lying triplet excited state T_3 (CT state for BBPI) and the HLCT S_1 state. While the T_3 of PhBPI is HLCT state with the CT S_1 state. In Figure 2, the calculated energy of the S_1 state (3.205 eV for BBPI and 3.115 eV for PhBPI) and the T_3 state (3.199 eV for BBPI and 3.102 eV for PhBPI) are almost same. So a little difference of singlet−triplet splitting can support a potential reverse intersystem crossing (RISC) from T_3 to S_1. Moreover, it can be seen the energy gap between the T_3 and the T_2 or T_1 states are more than 0.50 eV. Apparently, the internal conversion from the T_3 to the T_2 or T_1 states are smaller than the RISC from the T_3 to the S_1 states. Additionally, the transition from the T_1 to S_1 states is thought to be difficult due to the big energy difference (0.60 eV).

2.4. Electroluminescent (EL) Properties. To investigate the EL properties of BBPI and PhBPI, a construction of glass/indium tin oxide (ITO) (95 nm)/dipyrazino (2,3-f:2′,3′-h)-quinoxaline-2,3,6,7,10,11-hexacarbonitrile (HAT-CN) (5 nm)/*N*,*N*′-di-1-naphthyl-*N*,*N*′-diphenylbenzidine (NPB) (40 nm)/4,4′,4″-tri(*N*-carbazolyl)-triphenylamine (TCTA) (5 nm)/BBPI or PhBPI (20 nm)/1,3,5-tri(phenyl-2-benzimidazolyl)-benzene (TPBi) (40 nm)/LiF (1 nm)/Al (100 nm) is designed and fabricated, in which HAT-CN was utilized as a hole injection layer to improve the hole injection from the anode, NPB and TCTA are hole transport and electron block layer, respectively, TPBi is an electron transport layer, and LiF/Al is a bilayer cathode. Table 2 summarizes the important device parameters. As shown in Table 2, both devices based on BBPI and PhBPI have extremely low turn-on voltage (V_{on}) (at the luminance of 1 cd m^{-2}) and high efficiency. These two devices exhibit an excellent device efficiencies with maximal current efficiency (CE_{max}) of 6.8 and 5.5 cd A^{-1}, maximal power efficiency (PE_{max}) of 7.3 and 5.5 lm W^{-1}, respectively. They are among the best efficiencies of nondoped blue devices.[19,20]

Supporting Information Figure S7 presents the current density−voltage−luminance (*J*−*V*−*L*), current efficiency−luminance-power efficiency (CE−*L*−PE), luminance−external quantum efficiency (L−EQE) curves and EL spectrum. Compared with the devices with BBPI as eimtter, the *L*−*V* and *J*−*V* characterisitcs of the device based on PhBPI feature steeper increments, indicating the improved carrier injection and transport abilities. Otherwise, the device with BBPI as the emitting layer demonstrates much better performance than that with PhBPI as the emitting layer. In particular, the two devices show high maximum EQE of 6.1% and 4.2%. It is noteworthy that the EQE of the device with BBPI still reaches 5.6% when the luminance is up to 1000 cd/m^{-2}, which exhibits excellent performance with deep blue emission. The EQE values of the device based on BBPI apparently exceed the limited EQE of traditional fluorescent OLEDs, whose maximum EQE is only 5%, according to Monkman et al.[21] Furthermore, this value is generally estimated from the assumed fluorescence quantum yield (FLQY) 100%. Actually, the FLQY of PhBPI and BBPI films are 56.8% and 67.9%, respectively. Thus, the upper limit of the following equation:

$$\begin{aligned} EQE_{max} &= \eta_{op} \times \Phi_{fl} \times \eta_r \times \gamma \\ &\approx 0.2 \times \Phi_{fl} \times 0.25 \times 1 \\ &= 0.05\Phi_{fl} \end{aligned} \quad (1)$$

where η_{op} is the optical out coupling factor, Φ_{fl} is the fluorescence quantum yield, η_r is the possibility and γ is the charge balance factor. According to the values of Φ_{fl} of BBPI and PhBPI, the theoretical maximum EQE should be 3.40% and 2.84%. While the EQE can reach 6.1% and 4.2%, respectively. Then, one can figure out that the corresponding

Table 2. Summary of the Electroluminescent Performance of the Devices in a structure of ITO (95 nm)/HAT-CN (5 nm)/NPB (40 nm)/TCTA (5 nm)/Emitter (20 nm)/TPBi (40 nm)/LiF (1 nm)/Al (90 nm)

					at 100 cd m^{-2}					at 1000 cd m^{-2}				
emitter	V_{on}[a] (V)	CE_{max} (cd A^{-1})	PE_{max} (lm W^{-1})	EQE_{max} (%)	*V* (V)	CE (cd A^{-1})	PE (lm W^{-1})	CIE (*x*, *y*)	EQE (%)	*V* (V)	CE (cd A^{-1})	PE (lm W^{-1})	CIE (*x*, *y*)	EQE (%)
BBPI	2.6	6.8	7.3	6.1	3	6.8	7.3	(0.148, 0.140)	6.1	3.8	6.3	5.2	(0.147, 0.134)	5.6
PhBPI	2.7	5.5	5.5	4.2	3.2	5.5	5.3	(0.151, 0.149)	4.2	4.3	5.4	3.9	0.149, 0.145)	4.1

[a]At the luminance of 1 cd m^{-2}.

DOI: 10.1021/am5081106
ACS Appl. Mater. Interfaces 2015, 7, 7869−7877

internal quantum efficiency (IQE) should be 30.5% and 21.0%, and consequently, the exciton utilization efficiency (EUE) should be 44.9% and 37.0%, breaking through the limit of 25% according to spin statistics. As demonstrated above, these two molecules exhibit light emitting mechanism as HLCT. And thus, one can explain the light emitting mechanism as following Figure 3: 12.0% of triplet translate to singlet excitons by reverse

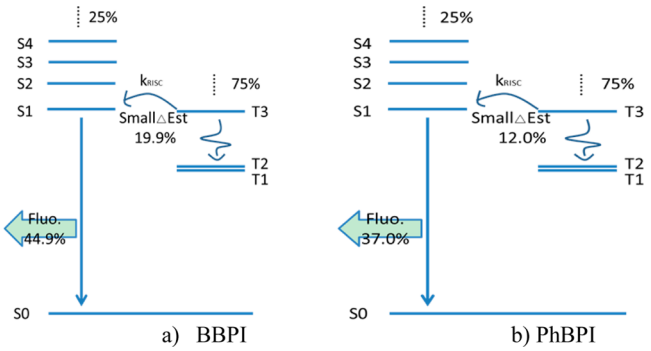

Figure 3. Illustration of exciton forming process of emitter from hole and electron recombination in electric excitation condition of OLEDs.

intersystem crossing progress to enhance the fluorescence emission, and the rest die away through nonradiative progress for PhBPI. As for BBPI, there are 19.9% of the triplet excitons translating to singlet excitons. This provides the possibility of high efficiency blue OLEDs.

Since the excellent blue OLED performance of BBPI or PhBPI with the characteristics of HLCT and "hot exciton", F/P hybrid WOLEDs with various phosphorescent dopant concentrations were constructed. The detailed device configuration is ITO (95 nm)/HAT-CN (5 nm)/NPB (80 nm)/TCTA (5 nm)/BBPI or PhBPI:*x* wt % $Ir(2\text{-phq})_3$ (20 nm)/ TPBi (40 nm)/LiF (1 nm)/Al (100 nm), in which *x* equals 0.1, 0.35, 0.6, or 1.0 wt %. In terms of these molecules with HLCT and "hot exciton" characteristic, thanks to part of triplet excitons translating to singlet ones, phosphorescent dopant concentration could be improved to a high level to achieve white light emission. Figure 4 gives the EL spectra of the BBPI/$Ir(2\text{-phq})_3$-based F/P hybrid WOLEDs at several typical luminance. As can be seen from Figure 4, the 0.1 wt % doped concentration cannot emit enough long wavelength phosphorescence even at the luminance of 100 cd m^{-2}. While the doped concentration was increased to 0.35 wt %, the CIE coordinates changed from (0.42, 0.36) to (0.28, 0.25) at the luminance range of 100 and 10000 cd m^{-2}. Thus, a cold white light can be obtained at high luminance. If the doped concentration was further increased to 0.6 wt %, the CIE coordinates changed from (0.47, 0.40) to (0.35, 0.30) at the practical luminance range of 100 and 10000 cd m^{-2}. In this case, we can get a near standard warm white light at high luminance. Even the doped concentration was increased to 1.0 wt %, the CIE coordinates changed from (0.51, 0.42) to (0.44, 0.37) at the same luminance range as above, indicating warm white OLEDs were fabricated. Meanwhile, the EL spectra of the PhBPI/$Ir(2\text{-phq})_3$-based F/P hybrid WOLEDs shows the similar results.

Figure 5 and Table 3 show the total efficiency characteristics and the summary of the electroluminescent performance of the F/P hybrid WOLEDs with BBPI acting as the blue emitter and the host of organe-red phosphorescent emitter. The WOLEDs have maximum total CE, PE, and EQE of 56.1 cd A^{-1}, 62.9 lm W^{-1}, and 23.8%, respectively. Even at the luminance of 1000 cd m^{-2}, the total CE, PE, and EQE remain to be 47.8 cd A^{-1}, 41.7

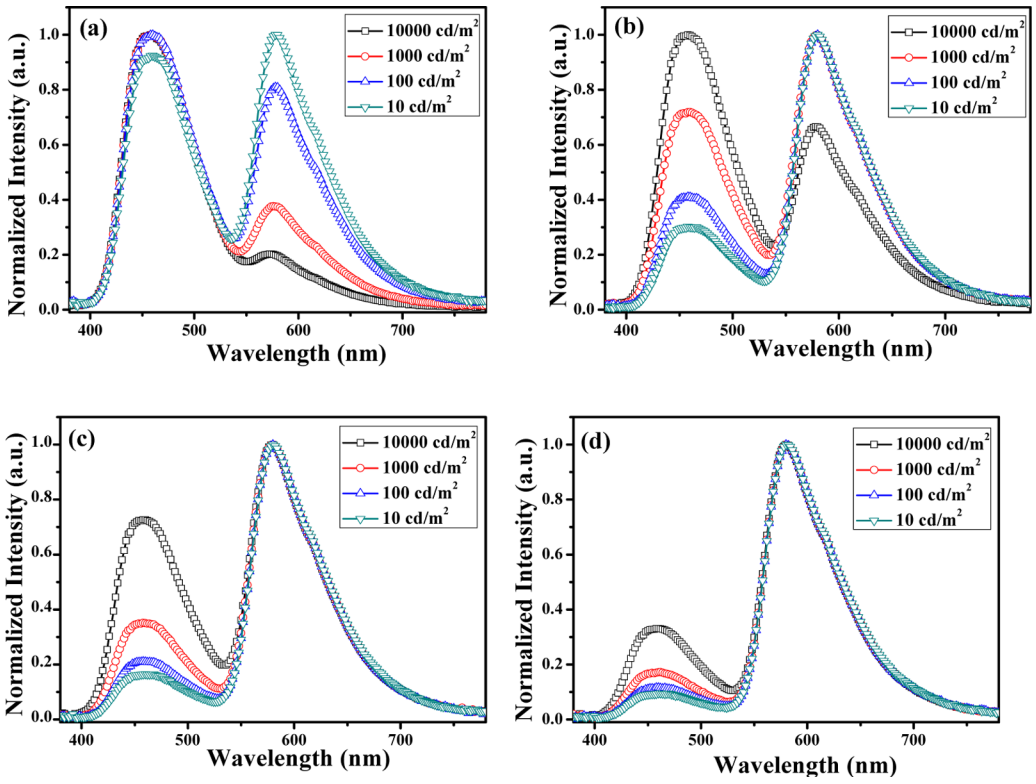

Figure 4. EL Spectra of the BBPI/*x* wt % $Ir(2\text{-phq})_3$-based F/P hybrid WOLEDs at different luminance and given doping concentrations of 0.1 (a), 0.35 (b), 0.6 (c), and 1.0 wt % (d).

DOI: 10.1021/am5081106
ACS Appl. Mater. Interfaces 2015, 7, 7869−7877

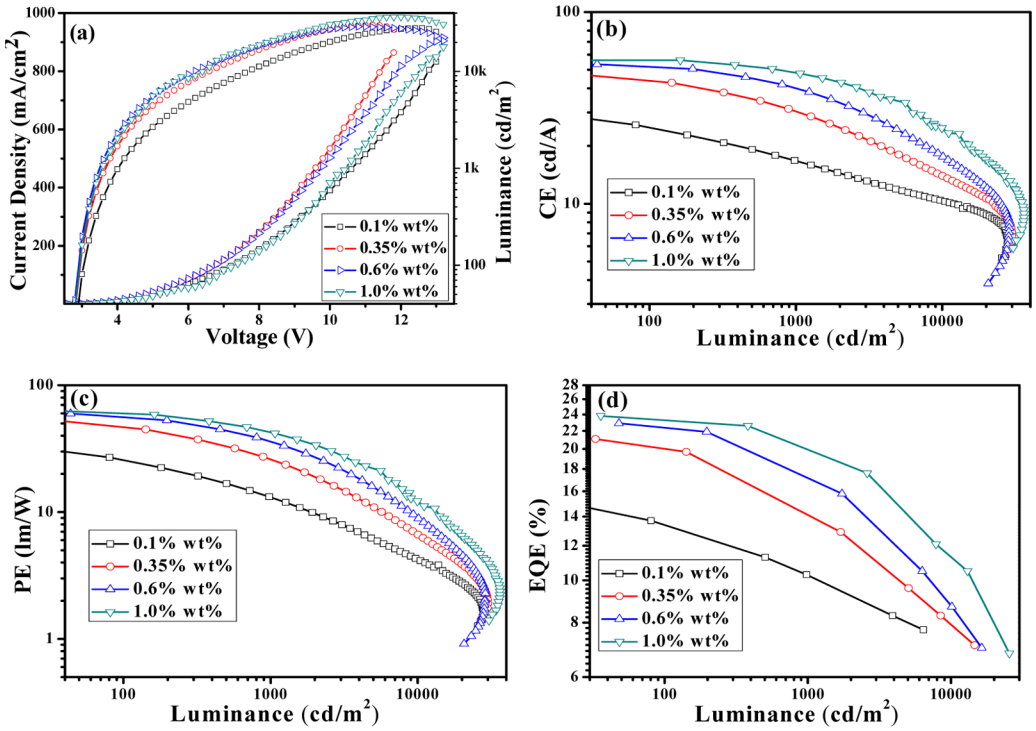

Figure 5. (a) *J*–*V*–*L*, (b) CE–*L*, (c) PE–*L*, and (d) *L*–EQE characteristics of the BBPI/Ir(2-phq)$_3$-based F/P hybrid WOLEDs at given doping concentrations.

Table 3. Summary of the Electroluminescent Performance of the Devices in a Structure of ITO (95 nm)/HAT-CN (5 nm)/NPB (40 nm)/TCTA (5 nm)/BBPI:*x* wt% Ir(2-phq)$_3$ (10 nm)/TPBi (40 nm)/LiF (1 nm)/ Al (90 nm)

					at 100 cd m^{-2}					at 1000 cd m^{-2}				
doping concentration	V_{on}[a] (V)	CE_{max} (cd A^{-1})	PE_{max} (lm W^{-1})	EQE_{max} (%)	*V* (V)	CE (cd A^{-1})	PE (lm W^{-1})	CIE (*x*, *y*)	EQE (%)	*V* (V)	CE (cd A^{-1})	PE (lm W^{-1})	CIE (*x*, *y*)	EQE (%)
0.10	2.6	31.8	38.4	15.1	3.1	24.7	24.7	(0.30, 0.27)	13.3	4.0	16.8	13.3	(0.23, 0.21)	10.2
0.35	2.6	47.3	52.9	21.1	3.0	42.3	44.7	(0.42, 0.36)	19.8	3.7	29.8	24.7	(0.37, 0.32)	14.3
0.6	2.6	53.4	59.8	22.9	2.9	51.9	55.8	(0.47, 0.40)	22.3	3.5	39.8	35.4	(0.45, 0.37)	17.3
1.0	2.6	56.1	62.9	23.8	2.9	56.1	60.4	(0.51, 0.42)	23.3	3.6	47.8	41.7	(0.49, 0.41)	20.1

[a]At the luminance of 1 cd/m^2.

lm W^{-1}, and 20.1%, respectively, at the dopant concentration of 1.0 wt %. While the concentration was decreased to 0.6 wt %, maximum total CE, PE, and EQE are 53.4 cd A^{-1}, 59.8 lm W^{1-}, and 22.9%, respectively. The total CE, PE, and EQE remain to be 39.8 cd A^{-1}, 35.4 lm W^{1-}, and 17.3%, respectively, at the luminance of 1000 cd m^{-2}. These are one of the best performances of SEML-SD F/P hybrid WLOEDs reported in the literature. F/P hybrid WOLEDs with PhBPI as the blue and the host of orange-red phosphorescent emitters were also fabricated in the same device structure, as exhibited in Supporting Information Figures S8 and S9 and Table S2. Likewise, the WOLEDs based on PhBPI have maximum total CE, PE, and EQE of 51 cd A^{-1}, 56.6 lm W^{-1}, and 21.9%, respectively. When the luminance is up to 1000 cd m^{-2} and the dopant concentration 1.0 wt %, the total CE, PE, and EQE remain to be 45.7 cd A^{-1}, 42.2 lm W^{-1}, and 18.9%, respectively. While the concentration is 0.6 wt %, maximum total CE, PE, and EQE are 45.6 cd A^{-1}, 51.2 lm W^{-1}, and 19.7%, respectively. By comparing with the performance of devices based on BBPI and PhBPI, it is obvious that the performance based on BBPI is better than that of PhBPI, which can be explain to be the high efficiency of BBPI for blue light.

2.5. Discussions about the Exciton Transfer in the High Phosphorescent Dopant Concentration Devices. Considering the low dopant concentration in the traditional single-EML-SD F/P hybrid WOLEDs, it is suspected that the current relatively high doping concentration should be resulted from the blue emitters with HLCT characters and thus "hot exciton" energy transfer from T_3 to S_1. Because of the part transfer from the triplet excited states to the singlet excited states of the blue emitter, the phosphorescent dopant cannot obtain sufficient energy to emit orange-red light of the traditional devices with the same doping concentration.[13,22] To get insight into the mechanism of exciton transfer, the transfer of the singlet excited states from blue fluorophore to phosphor should also be considered. As photoinduced excitons are all singlet ones, their photoluminescent spectra and transient PL with 1.0 wt % of Ir(2-phq)$_3$ were investigated with the same concentration as the fabricated WOLEDs. As Figure 6 (and Supporting Information Figure S10) demon-

DOI: 10.1021/am5081106
ACS Appl. Mater. Interfaces 2015, 7, 7869–7877

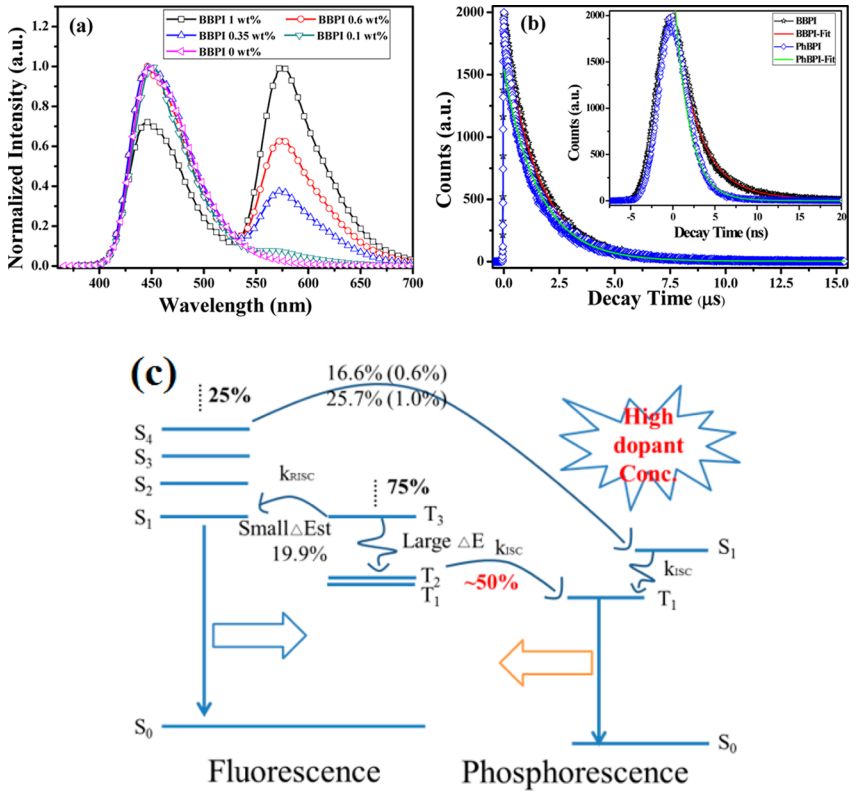

Figure 6. (a) PL spectra of the BBPI films doped with different concentrations of Ir(2-phq)$_3$. (b) Transient triplet PL of the BBPI and PhBPI films doped with 1.0 wt % of Ir(2-phq)$_3$, the corresponding transient singlet PL is shown in inserted figure. (c) The illustration of exciton forming process of emitter from hole and electron recombination in electric excitation condition of WOLEDs.

strates that the energy transfer from the singlet excited states of blue emitter to those of phosphorescent dopant is similar to the results in the literature,[13] while significant difference is observed in our WOLEDs. When the dopant concentration is 0.1 wt %, it cannot emit orange-red and only blue light. Only if the dopant concentration is up to 0.6 wt %, the present EL spectra are almost the same as those of the traditional ones at a doping concentration of 0.1 wt %. Even a further higher dopant concentration of 1.0 wt % still can emit sufficient blue and orange-red light to realize white light. To clearly illustrate the energy transfer of singlet excitons, the PL spectra are divided into those of the blue and orange-red components, as shown in Supporting Information Table S3, which means the ratio of the singlet excitons of the blue emitter that can be transferred to those of the orange-red ones. For the WOLEDs based on BBPI, when the doping concentration is 0.6 wt %, the singlet excitons on the blue part are found to be about 63.0%, implying about 28.3% of singlet excitons to emit blue light, while the corresponding energies of the triplet excitions, transferring directly from the triplet excited states of BBPI to those of Ir(2-phq)$_3$, are only 46.7% based on the EQE value of the devices. Likewise, as the doping concentration is increased up to 1.0 wt %, there are still 19.2% of the singlet excitons located at BBPI, the energy transfer from the triplet excited states of BBPI to those of Ir(2-phq)$_3$ is found to be only 50.3%. Meanwhile, as shown in Figure 6b, the triplet decay time of mixed film with BBPI and PBPI is about 1.57 μs, while the corresponding transient singlet lifetime is 2.67 ns for BBPI and 1.78 ns for PhBPI, respectively. The long singlet lifetime is better efficiency for fluorescent emission, it also means that the part triplet energy can be effectively transferred to singlet of fluorescent emitters. Accordingly, a more than 25% of triplet excitons cannot transfer from BPPI to Ir(2-phq)$_3$. It means that the insufficient energy can be transferred to the orange-red dopant, and the doping concentration should be improved to a high level. Furthermore, the present results can not only make the future mass production much easier to control accurately, but also a great breakthrough in the device mechanism, and then the design strategy.

3. CONCLUSION

In conclusion, a new design strategy has been demonstrated to obtain highly efficient single-EML-SD F/P hybrid WOLEDs. The key of this strategy is to employ the blue fluorophores with the ability to realize reverse intersystem crossing from the high-lying triplet excited states to the singlet excited states as the blue light emitter as well as the host of the orange-red phosphor. The diffusion volume range of the triplet excitons will be significantly reduced, and white light emission could even be achieved at a ten times higher phosphorescent dopant concentration compared with the traditional single-EML-SD F/P hybrid WOLEDs. Two such blue fluorophores with excellent HLCT and "hot exciton" properties were synthesized and used as the blue and the host of phosphorescent emitters. When the concentration of the phosphorescent dopant is up to 1.0 wt %, the device still shows a white emission with a low turn-on voltage of 2.6 V, total maximum CE of 56.1 cd A^{-1}, PE of 62.9 lm W^{-1}, and EQE of 23.8%. The current findings supply a novel way for obtaining high efficiency F/P hybrid WOLEDs in a SEML-SD architecture with easily controllable doping concentration.

DOI: 10.1021/am5081106
ACS Appl. Mater. Interfaces 2015, 7, 7869−7877

4. EXPERIMENTAL SECTION

4.1. General for the Synthesis and Materials. All chemical reagents were purchased from Sigma-Aldrich or Alfa Aesar and used directly. The specta of ^{1}H and ^{13}C NMR were measured on a Bruker AV-400. The elemental analyses of them were tested on a Vario EL elemental analysis instrument.

4.2. Route A. *4.2.1. Synthesis of Compound* ***1***. 4-Bromobenzaldehyde (0.185 g, 1.0 mmol), 0.208 g of phenanthrene-9,10-dione (1.0 mmol), 0.308 g of ammonium acetate (4.0 mmol), 0.465 g of aniline (5.0 mmol), and acetic acid (10 mL) were put into a flask and refluxed under nitrogen. After about 4 h, the reaction was stopped and cooled, and the mixture was added 50 mL of water and filtered. The precipitate was dissolved with dichloromethane and dried using anhydrous $MgSO_4$. Then, it was purified by column chromatography. ^{1}H NMR (400 MHz, DMSO): δ 7.53 (t, J = 7.8 Hz, 4H), 7.39−7.21 (m, 14H), 7.17 (t, J = 7.3 Hz, 1H). MS (ESI): 451.4, m/z 450.6 (M^+).

4.2.2. Synthesis of Compound ***PhBPI***. *N*,*N*-diphenyl-4′-(4,4,5,5-tetramethyl-1,3,2-dioxaborolan-2-yl)-[1,1′-biphenyl]-4-amine (2.235 g, 5.0 mmol), 2.135 g of compound **1** (4.8 mmol), and 50 mg of $Pd(PPh_3)_4$ (0.1 mmol) were added in the solution of 30 mL of toluene and 10 mL of 2 M K_2CO_3, and the mixture was heated to 105 °C and stirred for 16 h under nitrogen. After it was finished, the mixture was extracted by using CH_2Cl_2 (40 mL × 3 times), washed by using water (10 mL × 3 times), and dried with anhydrous $MgSO_4$. Then, the further purification was done by silica gel column chromatography with CH_2Cl_2−petroleum ether (60−90 °C) (2:1) as an eluent, a white solid was obtained. Yield: 0.45 g, 13.1%. ^{1}H NMR (400 MHz, $CDCl_3$): δ 8.95 (d, J = 7.86 Hz, 1H), 8.80 (d, J = 7.84 Hz, 1H), 8.74 (d, J = 8.84 Hz, 1H), 7.78 (t, J = 7.86 Hz, 1H), 7.71−7.61 (m, 10H), 7.60−7.52 (m,7H), 7.32−7.28 (m, 5H), 7.21 (d, J = 8.42 Hz, 1H), 7.18−7.16 (m, 6H), 7.06 (t, J = 7.68 Hz, 2H). ^{13}C NMR (100 MHz, $CDCl_3$): δ 147.6, 147.4, 141.0, 139.9, 138.6, 138.4, 134.3, 130.3, 130.0, 129.8, 129.4, 129.1, 128.3, 128.1, 127.6, 127.4, 127.3, 127.0, 126.7,126.3,155.8, 125.0, 124.5, 124.2, 123.8, 123.1, 123.0, 120.9. MS (EI): m/z 689.2 (M^+). Anal. Calcd for $C_{51}H_{35}N_3$: C, 88.79, H, 5.11, N, 6.1. Found: C, 88.71, H, 5.10, N, 6.16.

4.3. Route B. *4.3.1. Synthesis of Compound* ***2***. The synthesis of compound **2** followed the method of literature.[18] (4-(Diphenylamino)phenyl)boronic acid (2.89 g, 10.0 mmol), 1-bromo-4-iodobenzene (1.415 g, 5 mmol), and $Pd(PPh_3)_4$ (50 mg, 0.1 mmol) were suspended in toluene (30 mL) and 2 M K_2CO_3 (10 mL). The yield is 1.68 g and 84%. MS (EI): m/z 399.1, 401.3 (M^+).

4.3.2. Synthesis of Compound ***3***. Two grams of compound **2** (5 mmol), 0.75 g of 1-bromo-4-iodobenzene (5 mmol), and 50 mg of $Pd(PPh_3)_4$ (0.1 mmol) were added in a solution of 40 mL of toluene and 20 mL of 2 M K_2CO_3. The reaction was carried on at 105 °C for 24 h with the nitrogen atmosphere. The mixed solution was added to 20 mL, extracted by CH_2Cl_2 (40 mL × 3 times), and dried with anhydrous magnesium sulfate. After that, the mixture was purified with column chromatography by using CH_2Cl_2−petroleum ether (1:1). A yellow solid was obtained with yield of 1.83 g and 86.1%. ^{1}H NMR (400 MHz, $CDCl_3$): δ 10.01 (s, 4H), 7.99 (d, J = 7.86 Hz, 2H), 7.83 (d, J = 8.42 Hz, 2H), 7.75−7.70 (m, 4H), 7.55 (d, J = 8.42 Hz, 2H), 7.32−7.28 (m, 5H), 7.19−7.16 (m, 5H),7.07 (t, J = 7.86 Hz, 2H). MS (EI): m/z 425.2 (M^+).

4.3.3. Synthesis of Compound ***PhBPI***. The synthetic process of compound **PhBPI** is the same with the manner as compound **1**. Yield: 0.63 g, 91.4%. ^{1}H NMR (400 MHz, $CDCl_3$): δ 8.95 (d, J = 7.86 Hz, 1H), 8.80 (d, J = 7.84 Hz, 1H), 8.74 (d, J = 8.84 Hz, 1H), 7.78 (t, J = 7.86 Hz, 1H), 7.71−7.61 (m, 10H), 7.60−7.52 (m,7H), 7.32−7.28 (m, 5H), 7.21 (d, J = 8.42 Hz, 1H), 7.18−7.16 (m, 6H), 7.06 (t, J = 7.68 Hz, 2H). ^{13}C NMR (100 MHz, $CDCl_3$): δ 147.6, 147.4, 141.0, 139.9, 138.6, 138.4, 134.3, 130.3, 130.0, 129.8, 129.4, 129.1, 128.3, 128.1, 127.6, 127.4, 127.3, 127.0, 126.7,126.3,155.8, 125.0, 124.5, 124.2, 123.8, 123.1, 123.0, 120.9. MS (EI): m/z 689.2 (M^+). Anal. Calcd for $C_{51}H_{35}N_3$: C, 88.79, H, 5.11, N, 6.1; Found: C, 88.71, H, 5.10, N, 6.16.

4.4. Fabrication and Measurement of Devices. The EL devices were constructed by depositing the materials under the high vacuum. Before the fabrication of devices, the emitters of PhBPI and BBPI were purified deeply by sublimation. The functional and emitter layers were deposited onto a ITO with the resisitance of 20 Ω/m^2. A thin LiF (1 nm) was deposited between the cathode and organic layers. The L−V, J−V, and EL spectra were tested by a spectra scan spectrometer (PR705) and a a Keithley model 2420 programmable voltage−current source.

4.5. PL Measurements. The PL-containing fluorescent and phosphorescent spectrum were measuered on a Hitachi F-4500 fluorescence spectrometer. The target compounds were dissolved in tetrahydrofuran with the concentration of ∼10^{-7} mol/L. In order to test the phosphorescent emission, the solution should be cooled by using liquid nitrogen to 77 K. The lifetime of PL was tested on Edinburgh Instruments (FLS920) instrumtent.

4.6. Computational Details. The ground-state structures were optimized under the B3LYP/6-31G(d, p) level, which is well-known to provide molecular geometries in good agreement with the experiment. According to the optimized configuration of ground-state (S_0), the high excitation energy levels of singlet and triplet states were evaluated using TD-ωB97XD/6-31G (d,p). In order to find the characterization of excited-states, natural transition orbitals (NTOs) were evaluated for the lowest excited-states, involving both singlet and triplet states.

■ ASSOCIATED CONTENT

Supporting Information

Additional information contains TGA and DSC, absorption, and PL spectra with different solvents, phosphorescence spectrum, lifetime, and device performance. This material is available free of charge via the Internet at http://pubs.acs.org.

■ AUTHOR INFORMATION

Corresponding Authors

*E-mail: geziyi@nimte.ac.cn.
*E-mail: mssjsu@scut.edu.cn.

Author Contributions

X.O. and X.-L.L. contributed equally the paper.

Notes

The authors declare no competing financial interest.

■ ACKNOWLEDGMENTS

This work was financially supported from the National Natural Science Foundation of China (21102156, 51273209, 514111004, and 91233116). Z.Y.G. and X.O. greatly appreciate the financial support from the External Cooperation Program of the Chinese Academy of Sciences (No. GJHZ1219), Ningbo Natural Science Foundation (2014A610126), and Ningbo International Cooperation Foundation (2012D10009, 2013D10013). S.J.S. greatly appreciates the financial support from the Ministry of Education (NCET-11-0159) and the Department of Education of Guangdong Province (2012KJCX0008).

■ REFERENCES

(1) Su, S. J.; Gonmori, E.; Sasbe, H.; Kido, J. Highly Efficient Organic Blue-and White-Light-Emitting Devices Having a Carrier- and Exciton-Confining Structure for Reduced Efficiency Roll-Off. *Adv. Mater.* **2008**, *20*, 4189−4194.

(2) Gong, S. L.; Chen, Y. H.; Luo, J. J.; Yang, C. L.; Zhong, C.; Qin, J. G.; Ma, D. G. Bipolar Tetraarylsilanes as Universal Hosts for Blue, Green, Orange, and White Electrophosphorescence with High Efficiency and Low Efficiency Roll-Off. *Adv. Funct. Mater.* **2011**, *21*, 1168−1178.

(3) Li, G. J.; Fleetham, T.; Li, J. Efficient and Stable White Organic Light-Emitting Diodes Employing a Single Emitter. *Adv. Mater.* **2014**, *26*, 2931−2936.

DOI: 10.1021/am5081106
ACS Appl. Mater. Interfaces 2015, 7, 7869−7877

(4) Schwartz, G.; Reineke, S.; Rosenow, T. C.; Walzer, K.; Leo, K. Triplet Harvesting in Hybrid White Organic Light-Emitting Diodes. *Adv. Funct. Mater.* **2009**, *19*, 1319−1333.
(5) Sun, N.; Wang, Q.; Zhao, Y. B.; Chen, Y. H.; Yang, D. Z.; Zhao, F. C.; Chen, J. S.; Ma, D. G. High-Performance Hybrid White Organic Light-Emitting Devices without Interlayer between Fluorescent and Phosphorescent Emissive Regions. *Adv. Mater.* **2014**, *26*, 1617−1621.
(6) Zheng, C. J.; Wang, J.; Ye, J.; Lo, M.-F.; Liu, X. K.; Fung, M.-K.; Zhang, X. H.; Lee, C.-S. Novel Efficient Blue Fluorophors with Small Singlet-Triplet Splitting: Hosts for Highly Efficient Fluorescence and Phosphorescence Hybrid WOLEDs with Simplified Structure. *Adv. Mater.* **2013**, *25*, 2205−2211.
(7) Zhang, H. Y.; Huo, C.; Zhang, J. G.; Zhang, P.; Tian, W. J.; Wang, Y. Efficient Single-Layer Electroluminescent Device Based on a Bipolar Emitting Boron-Containing Material. *Chem. Commun.* **2006**, 281−283.
(8) Li, Z. H.; Wong, M. S.; Fukutani, H.; Tao, Y. Synthesis and Light-Emitting Properties of Bipolar Oligofluorenes Containing Triarylamine and 1,2,4-Triazole Moieties. *Org. Lett.* **2006**, *8*, 4271−4274.
(9) Yang, X. L.; Zhang, Y. B.; Zhang, X. W.; Li, R.; Dang, J. S.; Li, Y.; Zhou, G. J.; Wu, Z. X.; Ma, D. G.; Wong, W. Y.; Zhao, X.; Ren, A. M.; Wang, L. X.; Hou, X. Thiazole-Based Metallophosphors of Iridium with Balanced Carrier Injection/Transporting Features and Their Two-Colour WOLEDs Fabricated by both Vacuum Deposition and Solution Processing-Vacuum Deposition Hybrid Strategy. *J. Mater. Chem.* **2012**, *22*, 7136−7148.
(10) Sun, Y. R.; Giebink, N. C.; Kanno, H.; Ma, B. W.; Thompson, M. E.; Forrest, S. R. Management of Singlet and Triplet Excitons for Efficient White Organic Light-Emitting Devices. *Nature* **2006**, *440*, 908−912.
(11) Schwartz, G.; Fehse, K.; Pfeiffer, M.; Walzer, K.; Leo, K. Highly Efficient White Organic Light Emitting Diodes Comprising an Interlayer to Separate Fluorescent and Phosphorescent regions. *Appl. Phys. Lett.* **2006**, *89*, No. 083509.
(12) Baldo, M. A.; O'Brien, D. F.; Thompson, M. E.; Forrest, S. R. Excitonic Singlet-Triplet Ratio in a Semiconducting Organic Thin Film. *Phys. Rev. B* **1999**, *60*, 14422−14428.
(13) Ye, J.; Zhang, C. J.; Ou, X. M.; Zhang, X. H.; Fung, M.-K.; Lee, C.-S. Management of Singlet and Triplet Excitons in a Single Emission Layer: A Simple Approach for a High-Efficiency Fluorescence/Phosphorescence Hybrid White Organic Light-Emitting Device. *Adv. Mater.* **2012**, *24*, 3410−3414.
(14) Hu, J. Y.; Pu, Y. J.; Satoh, F.; Kawata, S.; Katagiri, H.; Sasabe, H.; Kido, J. Bisanthracene- Based Donor-Acceptor-type Light- Emitting Dopants: Highly Efficient Deep-Blue Emission in Organic Light-Emitting Devices. *Adv. Funct. Mater.* **2014**, *24*, 2064.
(15) Goushi, K.; Yoshida, K.; Sato, K.; Adachi, C. Organic Light-Emitting Diodes Employing Efficient Reverse Intersystem Crossing for Triplet-to-Singlet State Conversion. *Nat. Photonics* **2012**, *6*, 253−258.
(16) Li, W. J.; Liu, D. D.; Shen, F. Z.; Ma, D. G.; Wang, Z. M.; Feng, T.; Xu, Y. X.; Yang, B.; Ma, Y. G. A Twisting Donor−Acceptor Molecule with an Intercrossed Excited State for Highly Efficient, Deep-Blue Electroluminescence. *Adv. Funct. Mater.* **2012**, *22*, 2797−2803.
(17) Yao, L.; Zhang, S. T.; Wang, R.; Li, W. J.; Shen, F. Z.; Yang, B.; Ma, Y. G. Highly Efficient Near-Infrared Organic Light-Emitting Diode Based on a Butterfly-Shaped Donor−Acceptor Chromophore with Strong Solid-State Fluorescence and a Large Proportion of Radiative Excitons. *Angew. Chem., Int. Ed.* **2014**, *53*, 2119−2123.
(18) Ouyang, X. H.; Chen, D. C.; Zeng, S. M.; Zhang, X. Y.; Su, S. J.; Ge, Z. Y. Highly Efficient and Solution-Processed Iridium Complex for Single-layer Yellow Electrophosphorescent Diodes. *J. Mater. Chem.* **2012**, *22*, 23005−23011.
(19) Zhang, P.; Dou, W.; Ju, Z. H.; Yang, L. Z.; Tang, X. L.; Liu, W. S.; Wu, Y. Z. A 9,9′-Bianthracene-cored Molecule Enjoying Twisted Intramolecular Charge Transfer to Enhance Radiative-Excitons Generation for Highly Efficient Deep-Blue OLEDs. *Org. Electron.* **2013**, *14*, 915−925.
(20) Ouyang, X. H.; Zhang, X. Y.; Ge, Z. Y. Enhanced Efficiency in Nondoped, Blue Organic Light-Emitting Diodes Utilizing Simultaneously Local Excition and Two Charge-Transfer Exciton from Benzimidazole-Based Donor−Acceptor Molecules. *Dyes Pigm.* **2014**, *103*, 39−49.
(21) Chiang, C. J.; Kimyonok, A.; Etherington, M. K.; Griffiths, G. C.; Jankus, V.; Turksoy, F.; Monkman, A. P. Ultrahigh Efficiency Fluorescent Single and Bi-Layer Organic Light Emitting Diodes: The Key Role of Triplet Fusion. *Adv. Funct. Mater.* **2013**, *23*, 739−746.
(22) Yang, X. H.; Zheng, S. J.; Bottger, R.; Chae, H. S.; Tanaka, T.; Li, S.; Mochizuki, A.; Jabbour, G. E. Efficient Fluorescent Deep-Blue and Hybrid White Emitting Devices Based on Carbazole/Benzimidazole Compound. *J. Phys. Chem. C* **2011**, *115*, 14347.

DOI: 10.1021/am5081106
ACS Appl. Mater. Interfaces 2015, 7, 7869−7877